Journal of Research and Applications in Mechanical Engineering
ISSN: 2229-2152 (Print); 2697-424x (Online)
(2024) Vol. 12, No. 1, Paper No. JRAME-24-12-015
[DOI: 10.14456/jrame.2024.15]

*Research Article*

# Behavior of Plane Synthetic Jets Passing Over Two-Dimensional Flat Plates

**K. Suzuki**[1,*]
**K. Nishibe**[2]
**K. Sato**[3]
[1] *Mechanical Engineering Program in the Graduate School of Engineering, Kogakuin University, Tokyo 192-0015, Japan*
[2] *Department of Mechanical Engineering, Tokyo City University, Tokyo 158-8557, Japan*
[3] *Department of Mechanical System Engineering, Kogakuin University, Tokyo 192-0015, Japan*

**Received** 26 September 2023
**Revised** 26 November 2023
**Accepted** 4 December 2023

**Abstract:**
*Airflow control in railway and aircraft cabins, including air-conditioning and ventilation, is attracting increasing attention. Jet technology is typically employed for performing such controls. Synthetic jets, known for their inherent unsteadiness, have been investigated as an alternative to continuous jets, yielding diverse results. Researchers have endeavoured to elucidate the flow characteristics of synthetic jets in asymmetric flow fields. However, the relationship between the partition plate, which corresponds to a seat in a guest room, and jet flow remains unclear. Notably, studies investigating the flow characteristics when a partition plate is installed downstream of a synthetic jet are rare. In this study, the effects of a two-dimensional row of flat plates on the flow characteristics of a planar synthetic jet is investigated by installing multiple partition walls downstream of the slot. Flow visualization, velocimetry, and numerical simulations are performed, and the relationship between the recirculating flow and dimensionless frequency is discussed.*

**Keywords:** *Synthetic jet, Flat plates, Vortex, Frequency, CFD*

## 1. Introduction

The outbreak of COVID-19, which propagates through aerosol transmission, has triggered interest in improving ventilation, air-conditioning, and air purification systems in public transportation cabins. These cabins include those present in railcars, passenger aircraft, and buses. Generally, air outlets are strategically place at the front or near the ceiling of seats, while the air is often suctioned (discharged) from the rear of these seating areas. Therefore, knowledge concerning the flow control of jets passing through the flat rows of seats is essential for preventing the potential spread of viruses within these transportation environments.

The study of jet flow characteristics has been an active field for a long time [1, 2], and has yielded valuable insights. One well-known phenomenon in this field is the Coanda effect, where jets are attracted to a wall surface when an individual wall boundary surface exists near the jet. Consequently, the behaviours of wall-attached jets flowing on flat or cylindrical walls have been extensively investigated. More recently, synthetic jets have attracted considerable attention as promising alternatives to steady continuous jets, with multiple studies on synthetic jets having been already conducted [3-21]. Additionally, explorations into the behaviour of synthetic jets in asymmetric flow fields are also underway. For instance, Kobayashi et al. found the creating an asymmetric beak-shaped slot exit leads to the formation of a closed recirculation region in the flow field. Moreover, the shape depends on the dimensionless frequency and beak length [10]. Numerous other studies have focused on the flow characteristics of synthetic jets generated using asymmetric slots [11-15]. In addition, the basic flow characteristics of synthetic jets near a wall [5]

* Corresponding author: K. Suzuki
E-mail address: am23036@ns.kogakuin.ac.jp

and the peeling flow of synthetic jets on a cylindrical surface have also been discussed [16-21]. However, few fundamental studies exist regarding the development of these techniques. In particular, there is a scarcity of research on the flow characteristics of synthetic jets in situations where partition plates are installed downstream of the slot outlets.

Synthetic jets have an unsteady parameter "frequency", which does not exist in steady continuous jets. This study involves fundamental research for the application of synthetic jets to thermal management [22]. For example, we aim to control the airflow inside each cavity with the frequency without changing the geometry of the air outlet under the condition that the partition plates are placed near the air conditioning outlet, such as in a seat in a cabin. In particular, we attempt to elucidate the flow characteristics of a single plane synthetic jet with a row of two-dimensional flat plates placed near the slot. The effects of the dimensionless frequency on the flow characteristics have been unveiled by visualizing the flow, measuring the time-averaged velocity distribution, and examining the velocity vector and vorticity distribution using computational fluid dynamics (CFD) for various dimensionless frequencies under the same geometrical conditions.

## 2. Experimental Methods

Fig. 1 illustrates a schematic diagram of the apparatus used in the experiment. Panel (a) presents a top view, while panel (b) offers a side (front) view. Here, air is used as the working fluid. In this experiment, the test section was restrained by two 1.0 m×1.0 m acrylic plates to achieve 2D flow near the midspan. The slot height was $1.0\times10^{-1}$ m, and the aspect ratio to the slot width $b_0$ was 20. The measurement area extended across $4.0\times10^{-1}$ m along the x-axis direction and 1.0 m along the y-axis direction. To generate synthetic jets, speakers and Audacity, an audio editing software, were employed. These synthetic jets were shot in the rightward direction from the slot exit.

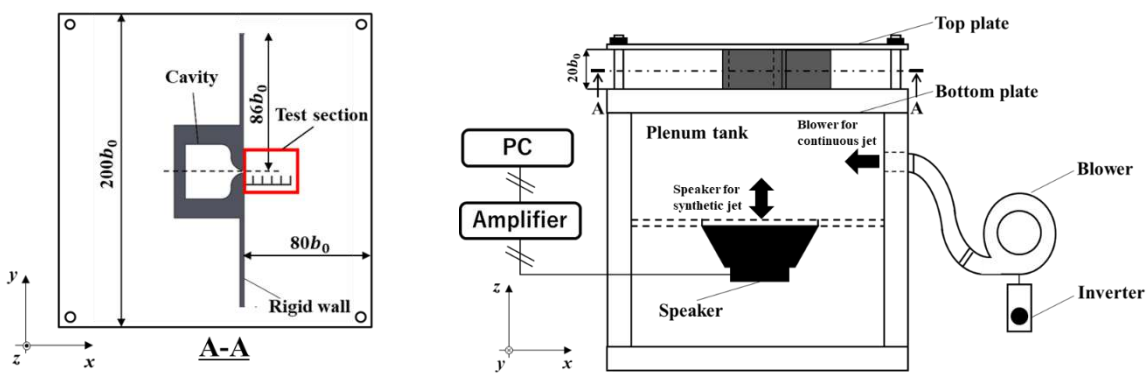


(a) Top View (b) Side view

**Fig. 1.** Experimental apparatus schematic diagram.

In this study, the representative velocity of the synthetic jet, $U_{S0}$ [m/s], was defined using the following equation, following the approach of Holman et al.:

$$U_{S0}=f\int_0^{\frac{T}{2}}u_0(t)dt \tag{1}$$

where $u_0$ is the velocity [m/s] at the slot exit, $T$ is the period [s], and $f$ is the frequency [Hz]. In this study, the flow velocity at the slot outlet was assumed to vary sinusoidally with time depending on the input signal, while the representative velocity was assumed to be constant at $U_{S0}$ = 4.5 m/s.

Fig. 2 provides a magnified view of the area near the slot exit. The slot width was set at $b_0 = 5.0\times10^{-3}$ m, and partition plates measuring $2.5\times10^{-2}$ m in height and $5.0\times10^{-3}$ m in width were placed at intervals of $2.5\times10^{-2}$ m. Additionally, a partition with a height of $5.0\times10^{-3}$ m and a width of $1.5\times10^{-1}$ m was placed at a distance $h = 4.0\times10^{-2}$ m from the slot center (with an offset ratio $H$ = 8).

Velocity measurements were conducted using a hot-wire anemometer (KANOMAX JAPAN, Inc. Smart CTA 7250) and a parallel flow probe (KANOMAX JAPAN, Inc. 0247R-T5). In the measurement range, the parallel flow probe was inserted from the top of the figure at $x/b_0$ = 2.5, 8.5, 14.5, 20.5, 26.5 with $y/b_0$ = -7.6~7.6 (at intervals of 2). For the flow visualization experiment, smoke was generated using the smoke wire method and captured using a digital camera operating at 480 fps. A laser (Kato Koken Co. Ltd. A PIV Laser G series) was employed as the light source.

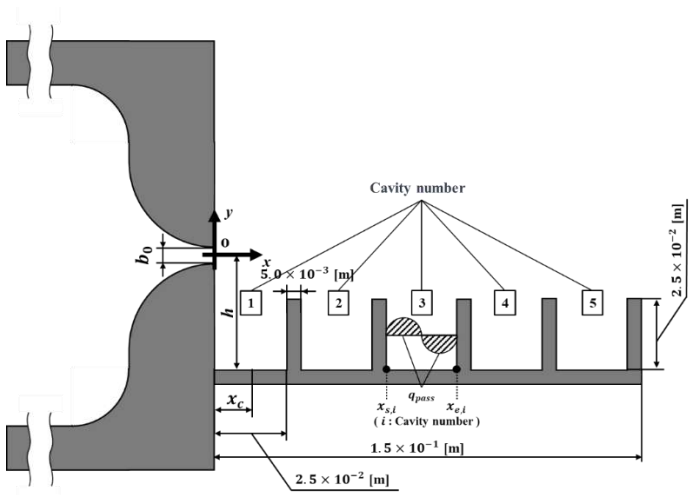


**Fig. 2.** Enlarged view of the slot test section.

## 3. Numerical Analysis conditions

Fig. 3(a) depicts the boundary conditions for the numerical calculations performed in this study, while Fig. 3(b) illustrates an example mesh near the slot. ANSYS 2021 R1 and Fluent (ANSYS, Inc.) were employed for the numerical calculations. The standard k-epsilon model was utilized as the turbulence model, with the numerical calculations performed assuming a 2D incompressible viscous flow. In terms of boundary conditions, aside from the non-slip wall surfaces, a flow velocity regulation was imposed on the inlet surface to ensure consistency with the flow velocity at the slot outlet. A static pressure condition was set at the outlet of the computational domain, and a total pressure condition was imposed for scenarios involving inflow. The number of meshes reached is approximately 110,000.

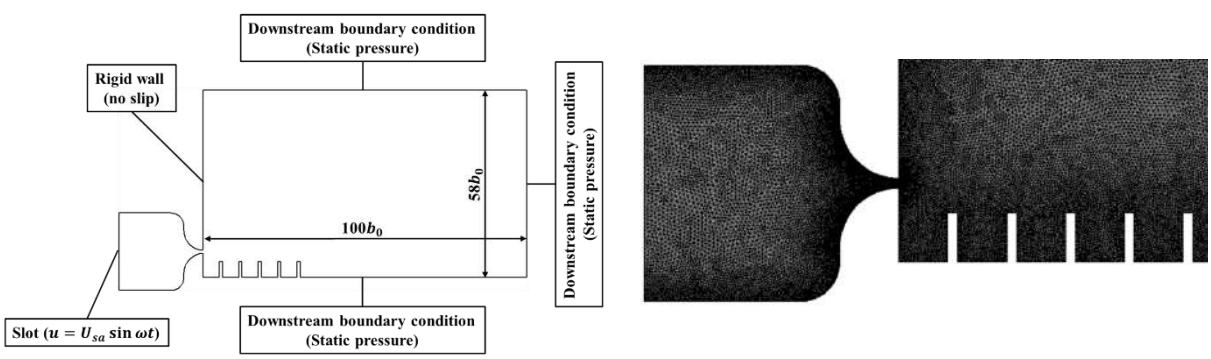


(a) Boundary condition (b) Mesh around the slot

**Fig. 3.** Boundary conditions and typical mesh for numerical analysis.

## 4. Results and Discussion

First, Fig. 4 shows a typical flow pattern for a continuous jet. Fig. 4(a) shows an example of the flow visualization obtained using the smoke wire method (frame rate 480 fps), and Fig. 4(b) shows the velocity vector and vorticity

distribution obtained from CFD. In Fig. 4(a), smoke flows into all the cavities, whereas in Fig. 4(b), the vorticity differs in each cavity, and in this condition, the vorticity in the central cavity No. 3 is larger than the others. Second, we focused our discussion on the flow field formed when the no-order frequency is $f^* = 0.033$ ($f = 30$ Hz). Fig. 5 presents examples of observed behaviour for (i) $t/T = 0$ ($u_0 = 0$), (ii) $t/T = 0.25$ (maximum jetting), (iii) $t/T = 0.50$ ($u_0 = 0$), and (iv) $t/T = 0.75$ (maximum suction) for one synthetic jet cycle. The time $t/T = 0$ marks the point when $u_0 = 0$ and the transition from the suction process to the ejection process takes place. Fig. 5(a) shows the visualization of the flow using the smoke wire method (red × and red arrows indicate the counterclockwise vortex centre and rotational direction, respectively; blue × and blue arrows represent the clockwise vortex centre and rotational direction, respectively). Fig. 5(b) shows the vorticity distribution and velocity vector outcomes obtained from the numerical simulation.

Upon comparing the experimental results depicted in (a) with the numerical results in (b), it becomes clear that there is qualitative agreement in the behaviour of the vortices. For instance, examining the jetting process from (i) to (iii), we can observe that in (ii), clockwise and counterclockwise vortex pairs form near the slot. Although the vortex pairs move in translation due to the induced velocity of each other, in (iii), there is a discrepancy in traveling velocity along the $x$ direction. This is due to the interference with the vortex generated within the cavity between the flat plates, resulting in the counterclockwise vortex taking the lead. Notably, the counterclockwise vortex in (iii) is observed to be ahead of the counterclockwise one owing to this interference within the cavity. In situations without a flat row of plates, the jet near the wall is attracted toward the wall owing to the Coanda effect. However, in the presence of a row of plates, the jet exhibits only a slight deflection toward the wall. In case (iv), the vortex continued to propagate despite the suction process. This can be attributed to the formation of vortex rows similar to a staggered array, although the vortex pairs were not symmetrical. The experimental results and the observed flow in the cavity between the plates confirmed the formation of vortices. In particular, the vorticity distribution of the numerical results (b) show that the counterclockwise vortex enters the cavity from (iii) to (iv), and the circulation region formed at $x/b_0$ =12~17 has the largest vorticity compared to the others. This suggests that by changing the dimensionless frequency, the stroke length (the length of the fluid mass ejected in one cycle) can be changed and vortices can be placed in arbitrary cavities.

Fig. 6 illustrates the distribution of the absolute time-averaged $x$-directional velocity, $|u|/U_{S0}$, for a continuous jet and a synthetic jet for $f^* = 0.033$, as measured by a hot-wire anemometer. The continuous jet is deflected toward the flat row (downward), which is similar to the behavior caused by the coanda effect observed in jets near a wall. In the case of the synthetic jet, it is confirmed that entrainment leads to the formation of a jet with a real flow rate even though the net flow rate is zero. Similar to the continuous jet, the synthetic jet is slightly attracted toward the flat row, as the flow moves downstream, the location of the maximum jet velocity shifts toward the negative direction of the $y$-axis because the jet is slightly attracted toward the flat row. Furthermore, because absolute values are shown in this figure, it is difficult to specify the direction of the flow. However, a comparison with the previous figure suggests that a large circulating flow is generated in the cavity near $x/b_0$ =14.5, which corresponds to the vorticity distribution shown in Fig. 5(b)(iii).

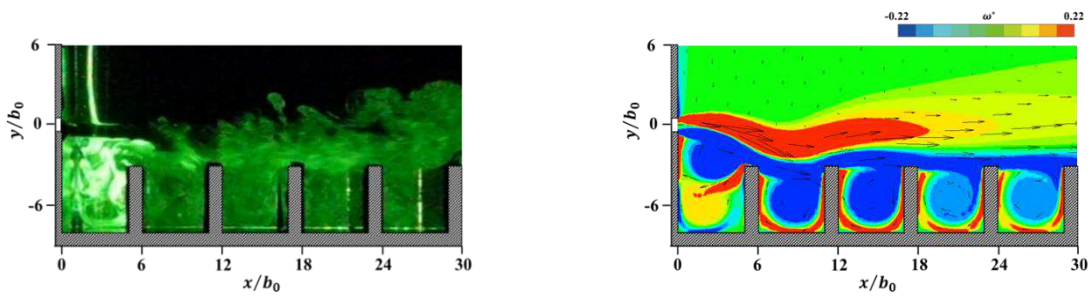


(a) Flow visualization by means of smoke wire method

(b) Vorticity contour and velocity vectors by CFD

**Fig. 4.** Flow pattern of the continuous jet obtained from experiment and CFD ($U_{C0} = 4.5$ m/s, $b_0 = 5.0\times10^{-3}$ m).

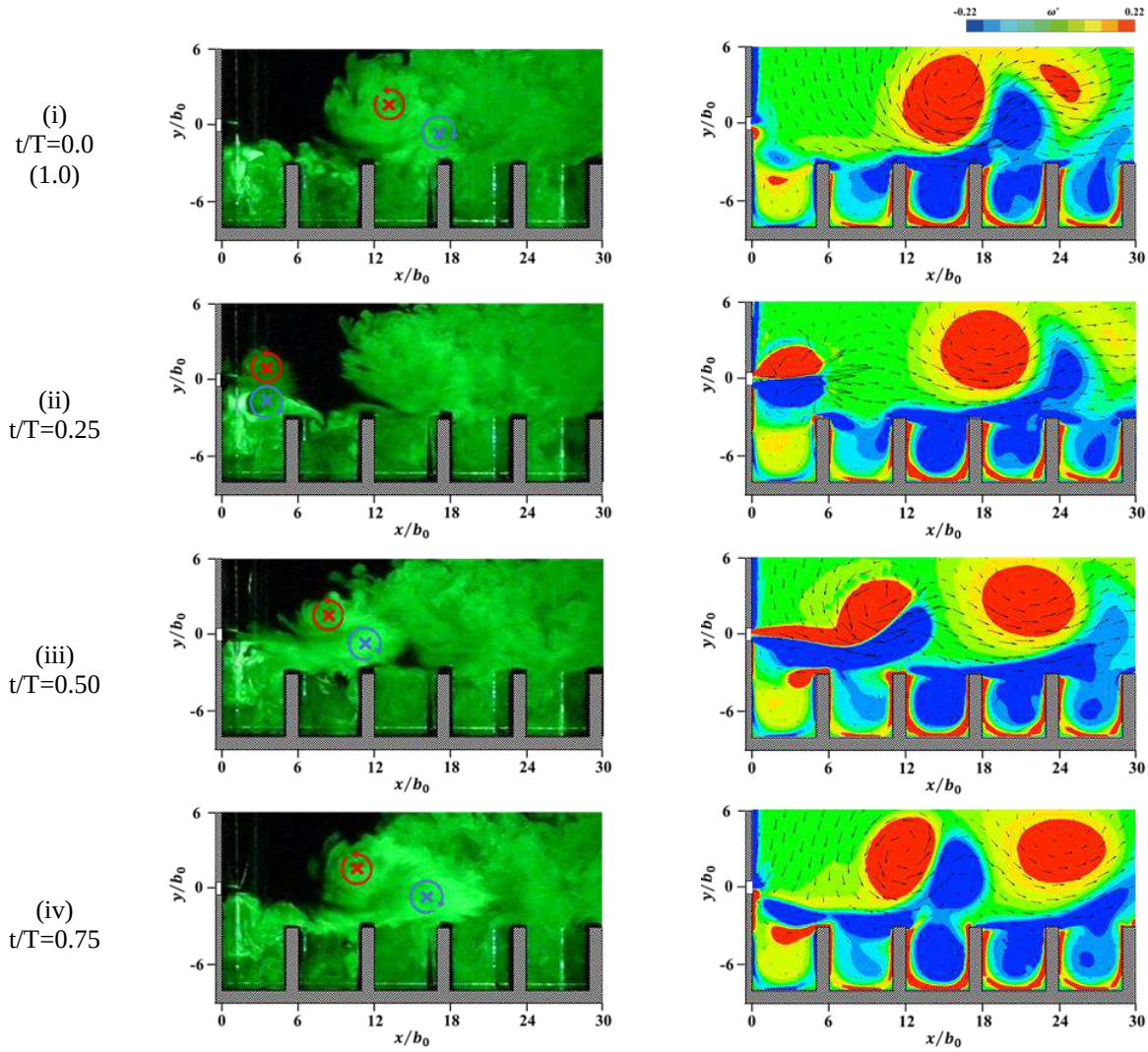


(a) Flow visualization by means of smoke wire method

(b) Vorticity contour and velocity vectors by CFD

**Fig. 5.** Temporal changes in flow pattern of the synthetic jet obtained from experiment and CFD ($U_{S0} = 4.5$ m/s, $f^* = 0.033$, $f = 30$ Hz, $b_0 = 5.0\times10^{-3}$ m).

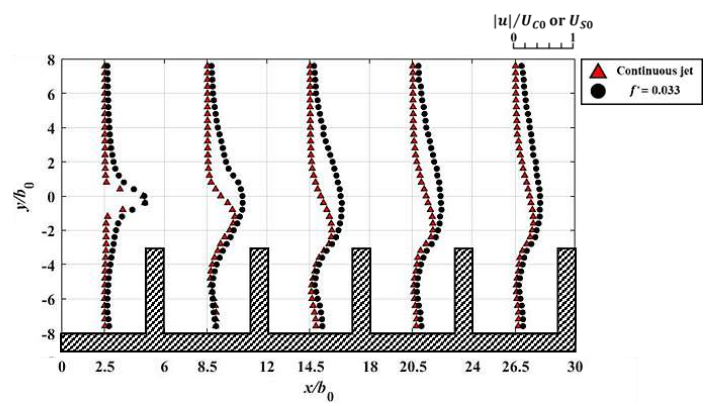


**Fig. 6.** Time-averaged velocity distributions obtained from experiment ($U_{S0} = 4.5$ m/s, $f^* = 0.033$, $f = 30$ Hz, $b_0 = 5.0\times10^{-3}$ m).

Fig. 7 depicts the time-averaged dimensionless flow $Q_{pass}$ ($=q_{pass}/q_0$) passing through the inspection plane $y/b_0$ =-5.5 positioned between each plate (in the cavity) for the continuous jet and various dimensionless frequencies obtained numerically. The parameter $Q_{pass}$ indicates the scale of the circulating flow inside a cavity. $q_{pass}$ is the absolute value of the velocity $v$ through the inspection surface integrated by $x$. It corresponds to the total flow rate across the inspection surface and, at the inspection surface location in this study, is considered to correspond to the intensity of recirculation in the cavity. For $q_0$, the product of the representative velocity, $U_{C0}$ or $U_{S0}$ (characteristic velocity at the slot exit), and the representative length, $b_0$ (slot width) was defined as the reference flow rate $q_0$. The value of $q_{pass}$ was measured by acquiring 26 $v$ points at intervals of $\Delta x$=1.0×10$^{-3}$ m at $y/b_0$ =-5.5 in each cavity. The following equation was then used for calculating $q_{pass}$:

$$q_{pass} = \int_{x_{s,\,i}}^{x_{e,\,i}} |v| dx \tag{2}$$

The abscissa is the dimensionless coordinate $x/b_0$ at the center between the plates, and the dimensionless frequency parameter is $f^*$ = 0.011, 0.033, 0.067 ($f$ = 10, 30, 60 Hz). The figure shows that the approximate shape of the curve depends on the jet configuration. For continuous jets, the cavities 3, 2, and 4 have larger values in that order. Conversely, for $f^*$ = 0.011 and 0.033, cavities 3, 4, and 2 have larger values in that order. Furthermore, when $f^*$ = 0.067, $Q_{pass}$ is the maximum at cavity No. 2 and decreases in the order of Nos. 3 and 4. In the synthetic jet, the dimensionless stroke length decreases as the dimensionless frequency increases; therefore, the upwind position of the vortex pair moves upstream. It can be inferred from this figure that the vortex upwind position was determined by the relative position between the vortex upwind position and the cavity created by the row of flat plates. Furthermore, this result suggests that the circulation scale of each cavity can be controlled to some extent by adjusting its dimensionless frequency.

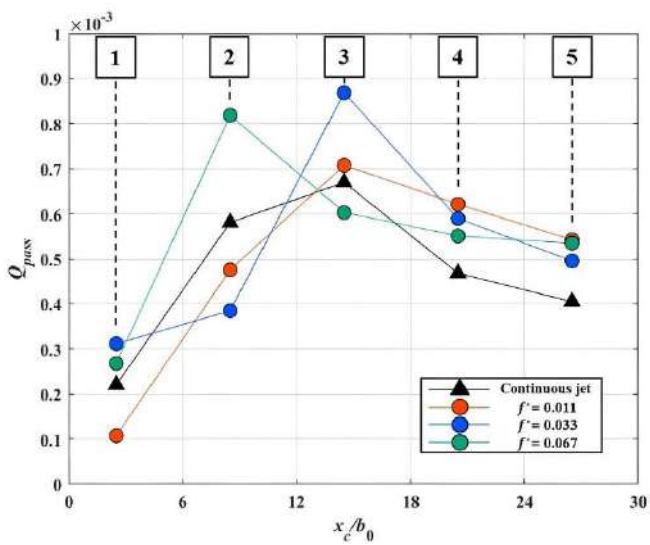


**Fig. 7.** Relationship between the position of the circulating vortex formed between the flat plates and the inflow flow rate obtained from CFD
($U_{C0} = U_{S0}$ = 4.5 m/s , $b_0$ = 5.0×10$^{-3}$ m).

## 5. Conclusion

This study, explores the flow characteristics in scenarios where a row of 2D flat plates is placed in the vicinity of a single planar synthetic jet. Flow visualization observations and time-averaged velocity profile measurements have been performed, alongside the presentation, of numerically calculated velocity vectors and vorticity profiles. The key findings of this study indicate that synthetic jets with real flow are formed in the vicinity of a 2D row of plates. Additionally, it has been observed that the vortex structure formed in the cavities

between the plates depends on the dimensionless frequency. These results suggest that it is possible to control the airflow in each cavity using dimensionless frequencies while maintaining the same geometrical conditions by applying synthetic jets as jets.

**Nomenclature**

| | |
|---|---|
| $b_0$ | Slot width (= $5.0\times10^{-3}$) [m] |
| $f$ | Frequency [Hz] |
| $f^*$ | Dimensionless frequency (=$fb_0/U_{S0}$) [-] |
| $h$ | Installation distance of flat plate row [m] |
| $H$ | Offset ratio (=$h/b_0$) [-] |
| $i$ | Cavity number |
| $l_0$ | Stroke length (=$U_{S0}/f$) [m] |
| $L_0$ | Dimensionless stroke length ($U_{S0}/fb_0$) [-] |
| $q_{pass}$ | Flow rate through the inspection surface in each cavity (= $\int_{x_{s,\,i}}^{x_{e,\,i}}\|v\|dx$) |
| $q_0$ | Reference flow rate (=$b_0U_{S0}$ or $b_0U_{C0}$ ) |
| $Q_{pass}$ | Dimensionless flow in each cavity (=$q_{pass}/q_0$) [-] |
| $Re$ | Reynolds number (=$U_{C0}b_0/\nu=U_{S0}b_0/\nu$=1500) [-] |
| $t$ | Time [s] |
| $T$ | Period of velocity oscillation at slot exit [s] |
| $u$ | Velocity in the $x$-direction [m/s] |
| $u_0$ | Velocity in the $x$-direction at the slot exit [m/s] |
| $U_{C0}$ | Characteristic velocity in continuous jets [m/s] |
| $U_{S0}$ | Characteristic velocity in synthetic jets [m/s] |
| $v$ | Velocity in the $y$-direction [m/s] |
| $x, y, z$ | Coordinate axes |
| $x_c$ | $x$ component of the center coordinate between each flat plate [m] |
| $\nu$ | Kinematic viscosity (= $1.5\times10^{-5}$) [$m^2/s$] |
| $\omega$ | Vorticity [1/s] |
| $\omega^*$ | Dimensionless vorticity (=$\omega b_0/U_{C0}=\omega b_0/U_{S0}$) [-] |

**Acknowledgments**

This work was supported by JSPS KAKENHI Grant Number 23K17731 and Hatakeyama Research Grant of Turbomachinery Society of Japan.

**References**

[1] Neuendorf R, Wygnanski I. On a turbulent wall jet flowing over a circular cylinder. J Fluid Mech. 1999;381:1-25.
[2] Shakouchi T. Jet Flow engineering. Tokyo: Morikita Publishing; 2004.
[3] Holman R, Utturkar Y, Mittal R, Smith BL, Cattafesta L. Formation criterion for synthetic jets. AIAA J. 2005;43(10):2110-2116.
[4] Smith BL, Swift GW. A comparison between synthetic jets and continuous jets. Exp Fluids. 2003;34(4):467-472.
[5] Nishibe K, Fujita Y, Sato K, Yokota K, Koso T. Experimental and numerical study on the flow characteristics of synthetic jets. J Fluid Sci Technol. 2011;6(4):425-436.
[6] Nishibe K, Nomura Y, Noda K, Ohue H, Sato K. Influence of stroke on performance characteristics of synthetic jet fan. J Appl Fluid Mech. 2018;11(4):945-956.
[7] Koso T, Morita M. Effects of stroke and Reynolds number on characteristics of circular synthetic jets. J Fluid Sci Technol. 2014;9(2):1-15.
[8] Koso T, Matsuda S, Masuda H, Akahoshi T. Effect of stroke on structure of vortex ring array in circular synthetic jets. J Fluid Sci Technol. 2014;9(3):1-11.

[9] Yasumiba M, Nishibe K, Kang D, Sato K. Flow characteristics of two-dimensional impinging synthetic jets. J Energy Syst. 2023;7(4):327-338.
[10] Kobayashi R, Nishibe K, Watabe Y, Sato K, Yokota K. Vector control of synthetic jets using an asymmetric slot. J Fluids Eng. 2018;140(5):051102.
[11] Kobayashi R, Terakado H, Sato K, Taniguchi J, Nishibe K, Yokota K. Behavior of plane synthetic jets generated by an asymmetric stepped slot. Int J Fluid Mach Syst. 2020;13(1):253-265.
[12] Terakado H, Nishibe K, Kang D, Yokota K, Sato K. Behavior of synthetic jets in an asymmetric flow field. The 6th International Conference on Jets, Wakes and Separated Flows (ICJWSF2017); 2017 Oct 9-12; Cincinnati, United States.
[13] Kawahara R, Kobayashi R, Sato K, Nishibe K, Yokota T. Influence of stepped slot geometry on the deflection of synthetic jets. Proceedings of 31st International Symposium on Transport Phenomena; 2020 Oct 13-16; Online.
[14] Ito T, Miyachi Y, Nishibe K, Sato K. Influence of rectangular protrusion-shaped slot on flow characteristics of synthetic jets. In the 7th International Conference on Jets, Wakes and Separated Flow (ICJWSF2022); 2022 Mar 15-17; Online.
[15] Ito T, Nishibe K, Sato K, Kang D. Influence of asymmetric protrusion-shaped slots on synthetic jets. The 32nd International Symposium on Transport Phenomena; 2022 Mar 19-21; Tianjin, China.
[16] Kobayashi R, Watanabe Y, Tamanoi Y, Nishibe K, Kang D, Sato K. Jet vectoring using secondary Coanda synthetic jets. Mech Eng J. 2020;7(5):1-17.
[17] Zhang Q, Tamanoi Y, Kang D, Nishibe K, Yokota K, Sato K. Influence of amplitude of excited secondary flow on the direction of jets. Trans Japan Soc Aero Space Sci. 2023;66(2):37-45.
[18] Tezuka H, Zhang Q, Nishibe K, Sato K. Flow-direction control of primary jets near a wall boundary using secondary flow with a coanda surface. J Res Appl Mech Eng. 2023;11(2):1-7.
[19] Okada T, Hiruma T, Nishibe K, Sato K. Flow characteristics of synthetic jet near curved wall. Proceedings of the 9th World Congress on Mechanical, Chemical, and Material Engineering (MCM'23); 2023 Aug 6-8; London, United Kingdom.
[20] Sakakura T, Yamaguchi K, Nishibe K, Ohue H, Sato K. Influence of stroke on jet structure of wall-synthetic jet flowing over circular cylinder. The 31st International Symposium on Transport Phenomena; 2020 Oct 13-16; Online.
[21] Yamaguchi K, Sakakura T, Nishibe K, Ohue H, Sato K. Jet structure of plane and curved wall-synthetic jet. The 31st International Symposium on Transport Phenomena; 2020 Oct 13-16; Online.
[22] Krishan G, Aw KC, Sharma RN. Synthetic jet impingement heat transfer enhancement: a review. Appl Therm Eng. 2019;149:1305-1323.